In vitro selection of a novel nuclease-resistant RNA phosphodiesterase

Amber Beaudry[1], James DeFoe[1], Shawn Zinnen[1], Alex Burgin[2] and Leonid Beigelman[1]

Background: Ribonucleotide-based enzymes (ribozymes) that cleave pathological RNAs are being developed as therapeutic agents. Chemical modification of the hammerhead ribozyme has produced nuclease-resistant catalysts that cleave targeted mRNAs in cell culture and exhibit antitumor activity in animals. Unfortunately, stabilizing modifications usually reduce the catalytic rate *in vitro*. An alternative to rationally designed chemical modifications of existing ribozymes is to identify novel motifs through *in vitro* selection of nuclease-stable sequence space. This approach is desirable because the catalysts can be optimized to function under simulated physiological conditions.

Results: Utilizing *in vitro* selection, we have identified a nuclease-stable phosphodiesterase that demonstrated optimal activity at simulated physiological conditions. The initial library of 10^{14} unique molecules contained 40 randomized nucleotides with all pyrimidines in a nuclease-stabilized 2′-deoxy-2′-amino format. The selection required *trans*-cleaving activity and base-pairing specificity towards a resin-bound RNA substrate. Initial selective pressure was permissive, with a 30 min reaction time and 25 mM Mg^{2+}. Stringency of selection pressure was gradually increased until final conditions of 1 mM Mg^{2+} and less than 1 min reaction times were achieved. The resulting 61-mer catalyst required the 2′-amino substitutions at selected pyrimidine positions and was stable in human serum (half-life of 16 h).

Conclusions: We demonstrated that it is possible to identify completely novel, nuclease-resistant ribozymes capable of *trans*-cleaving target RNAs at physiologically relevant Mg^{2+} concentrations. The new ribozyme motif has minimal substrate requirements, allowing for a wide range of potential RNA targets.

Addresses: [1]Department of Biochemistry, Ribozyme Pharmaceuticals, 2950 Wilderness Place, Boulder CO 80301, USA. [2]Department of Biology, San Diego State University, San Diego, CA 92182-4614, USA.

Correspondence: Leonid Beigelman
E-mail: LNB@rpi.com

Key words: 2′-deoxy-2′-aminopyrimidine RNA, catalytic RNA, *in vitro* selection, ribozymes, RNA therapeutics

Received: **26 November 1999**
Revisions requested: **6 January 2000**
Revisions received: **16 February 2000**
Accepted: **23 February 2000**

Published: **18 April 2000**

Chemistry & Biology 2000, **7**:323–334

1074-5521/00/$ – see front matter

Introduction

The ability of catalytic RNA [1,2] to specifically bind and cleave other RNAs has been recognized as method of controlling gene expression [3]. The hammerhead ribozyme, being the smallest natural phosphodiesterase, has been chemically modified to function in a therapeutic setting [4,5]. This stabilization increased nuclease resistance while maintaining catalytic activity and has produced ribozymes capable of down-regulating gene expression *in vitro* and *in vivo* [6–9]. Several stabilized hammerhead ribozymes are currently being evaluated in human clinical trials [8].

The discovery of catalytic RNA has also generated a search for new ribozymes of natural origin (for reviews, see [10–12]) that may also have therapeutic value, and challenged scientists to find ribozymes capable of catalyzing a diverse set of chemical reactions [13–16]. *In vitro* selection has been used to develop new catalysts or optimize existing ribozymes [17–19]. For example, attempts have been made to select from libraries ribozymes containing features of the hammerhead [20–26]. These selections have been done in an all-ribonucleotide format and have therefore required subsequent nuclease stabilization. Stabilizing chemical modifications, with rare exceptions [27,28], cause a decrease in the cleavage rate *in vitro* [4,5]. Other selections have been performed and have identified an AUG-cleaving hammerhead-like ribozyme as a new purine-specific ribozyme motif [29]. It remains to be seen whether this ribozyme will be amenable to stabilizing chemical modifications.

The need to identify chemically stable nucleic acid catalysts led to the development of the first deoxyribonucleotide catalyst [30]. It was shown that a 14-mer oligodeoxynucleotide could catalyze the cleavage of a 35-mer RNA substrate, but with lower catalytic efficiency than partially substituted hammerhead ribozymes. This was followed by the discovery that DNA could perform phosphodiester cleavage of RNA in the presence of Pb^{2+}

[31], and led to the selection and characterization of magnesium-dependent DNA enzymes [32,33]. The smallest of these is 31 deoxynucleotides and cleaves RNA *in trans* with k_{cat}/K_m in the range of 10^8 M^{-1} min^{-1} at 2 mM $MgCl_2$ [34]. Application of this motif in cell culture has shown specific knockdown of target mRNA in model systems [35–37]. Although DNA is generally less sensitive to nuclease degradation, unmodified DNA enzymes were broken down in 10% fetal bovine serum and in human serum [34,35,37]. Chemical modifications increased the extent of protection from degradation and have been shown to be effective in cell culture models.

We designed a selection that explored nuclease-stable sequence space by using 2′-deoxy-2′-aminopyrimidine nucleotides. The selective pressures required *trans*-cleavage and were moved towards physiological ion concentrations. A novel non-hammerhead-like ribozyme with inherent nuclease stability and optimal activity under physiological conditions was generated. To the best of our knowledge, this is the first demonstration that nuclease-resistant ribozymes can be directly evolved through an *in vitro* selection approach.

Results and discussion

In vitro selection scheme and initial selection of active pool

We designed a selection scheme to mimic what is required of a therapeutic ribozyme *in vivo*: bind the target RNA through specific base-pairing interactions and, in a *trans* reaction, cleave the target RNA under physiological conditions. 2′-deoxy-2′-aminopyrimidine nucleotides were used to generate a chemically stabilized RNA sequence pool. The initial pool (N = 40) contained 3×10^{14} individual sequences transcribed using a T7 RNA polymerase with 2′-amino-dCTP/2′-amino-dUTP and normal ATP/GTP. To increase the amount of this modified RNA product, transcription conditions were optimized by inclusion of methanol [38] and lithium chloride in the reaction buffer. The 2′-amino-2′-deoxynucleotides do not interfere with the reverse transcription and amplification steps of selection and confer nuclease resistance [39]. This inherent nuclease resistance offers an advantage over unmodified hammerhead ribozymes and DNA enzymes, while also allowing for unique tertiary interactions not possible with 2′-OH or 2′-H.

We designed the RNA in the pool to have two binding arms, complementary to a specific substrate RNA, separated by 40 random nucleotides (Figure 1). The 16-mer substrate had two binding domains, 5 and 10 nucleotides long, separated by an unpaired guanosine. The two binding domains in the substrate RNA bind to the two binding arms in the pool to form 15 base pairs (5/10). The 5′-end of the substrate had a biotin molecule attached through a C18 linker. The substrate was linked to a NeutrAvidin resin and the selection was performed in a column format [22]. The desired reaction was cleavage at the unpaired G upon addition of magnesium. Subsequent instability of the product (five base pair helix) allowed dissociation from the column. The predicted dissociation constant at 37°C ($K_d^{37°C}$) for dissociation of an active species with the 5′-portion of cleaved substrate was calculated to be 43 μM, whereas the predicted $K_d^{37°C}$ for any member of the random population to hybridize to the 16-mer substrate is 2×10^{-8} nM [40]. The actual $K_d^{37°C}$ could differ because the 2′-amino modification confers decreased thermodynamic stability in duplex formation [41], so we performed model experiments to characterize column behavior. After the substrate was linked to the column, the pool was added in column buffer (50 mM Tris–HCl, pH 8.5, 100 mM NaCl, 50 mM KCl) and allowed to bind. The column was washed until the amount of pool coming off the column was reduced to background levels. More than 60% of the initial pool was bound at this point. Incubation with elution buffer containing 25 mM $MgCl_2$ for 30 min resulted in background levels of pool coming off the column; we thus believed that the binding of pool to substrate was stable. The pool bound to the column could then be eluted using 7 M urea, indicating that the binding is reversible. A control column with no substrate linked was run in parallel and showed that the column binding is specific to the presence of substrate. Pool 'eluted' following the incubation with $MgCl_2$ was precipitated, amplified and transcribed as described in the Materials and methods section. This constitutes one round of selection. Initially, selection was done with permissive cleavage conditions

Figure 1

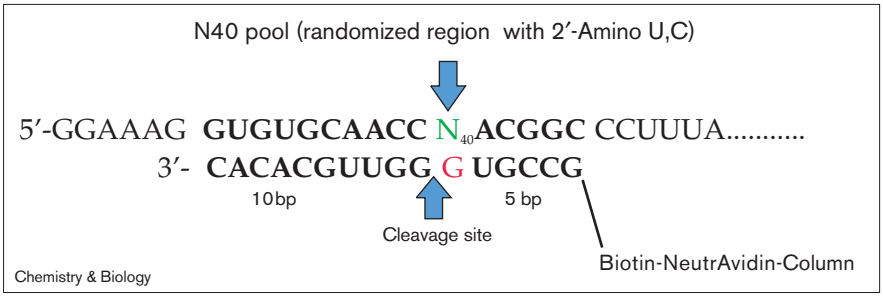

Scheme for 2′-amino-dCTP/dUTP *trans* selection. Randomized RNA pool with engineered binding arms is allowed to base pair with column-bound substrate. Exposure to magnesium allows for potential cleavage of substrate at unpaired G and dissociation from column.

(25 mM Mg^{2+}, pH 8.5, 100 mM NaCl, 50 mM KCl, 30 min, 25°C). This allowed the presumably small number of catalysts with any cleavage activity to survive the selection. The selection conditions were then made more stringent to identify catalysts with robust catalytic efficiencies under physiological conditions.

After eight rounds of selection, we saw no activity in a single turnover kinetic assay (under the selection conditions of 25 mM $MgCl_2$, 50 mM Tris–HCl, pH 8.5, 100 mM NaCl, 50 mM KCl). We decided to make the selection more stringent. We modified the substrate such that the 10-base-pair interaction between one of the binding arms of the RNA pool and substrate became 16 base pairs (5/16) and, therefore, binding was made more stable. The K_d measured by gel-shift assay went from 31 nM (5/10) to 3 nM (5/16); the K_d of one of the product pieces alone (16-mer) was 4 nM (data not shown). Because product dissociation is expected to be slow, ribozymes that come off the column as a result of a cleavage event would stay bound to its 3′ product (16-mer). The eluent was then passed through an additional 'product' column that had the 16 nucleotide 3′ fragment of substrate attached through the same chemistry as original substrate. It was anticipated that this column would bind any individual that was eluted from the first column through a noncleavage event (i.e. dissociation), whereas ribozyme with clevage product bound should flow through. This eluent was precipitated and amplified as previously described. After three more rounds in this format (generation 11), there was visible activity in a single turnover cleavage assay (3% cleaved at 4 h, Figure 2). By generation 13 (G13), 45% of the substrate was cleaved at 4 h; the observed rate constant (k_{obs}) of the pool was 0.037 min^{-1} in 25 mM $MgCl_2$. We subcloned and sequenced G13; the pool was still very diverse (data not shown). Because our goal was to obtain a ribozyme that would work in a physiological environment, we decided to change selection pressure rather than exhaustively catalog G13 members.

Optimization of initial active pool at physiological conditions

Optimization of the N40 pool was started from the G12 DNA pool. Part of the G12 pool DNA was subjected to hypermutagenic PCR [42] to introduce a 10% per position mutation frequency and was designated N40H. At round 19, part of the DNA was hypermutagenized again, giving N40M and N40HM (a total of four parallel pools). The column substrates remained the same; temperature of binding and elution was raised to 37°C. Column buffer was replaced by physiological buffer (50 mM Tris–HCl, pH 7.5, 140 mM KCl, 10 mM NaCl) and elution buffer was replaced by 1 mM Mg buffer (physiological buffer +1 mM $MgCl_2$). The amount of time allowed for the pool to bind to the column was eventually reduced to 10 minutes and elution time was gradually reduced from 30 minutes to 20 seconds (Figure 3). Between rounds 18 and 23, k_{obs} for the initial N40 pool stayed relatively constant at 0.035–0.04 min^{-1}. At generations 21–22, all four pools started to display similar k_{obs} values (0.035–0.04 min^{-1}), indicating that the selection was complete. G22 from each of the four pools was cloned and representative members

Figure 2

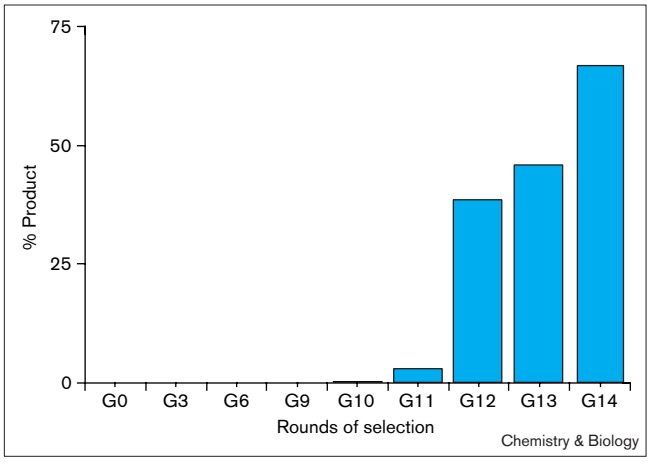

Progress of initial selection as measured by the cleavage assay. Pools were incubated under single-turnover conditions with labeled substrate and quenched after 4 h. Amount of substrate converted to product is shown. G, generation; reaction conditions: 50 mM Tris–HCl, pH 8.5, 100 mM NaCl, 50 mM KCl, 25 mM $MgCl_2$, 37°C, 10 nM pool, < 1 nM substrate (5′-^{32}P-GCC GUG GGU UGC ACA C-3′).

Figure 3

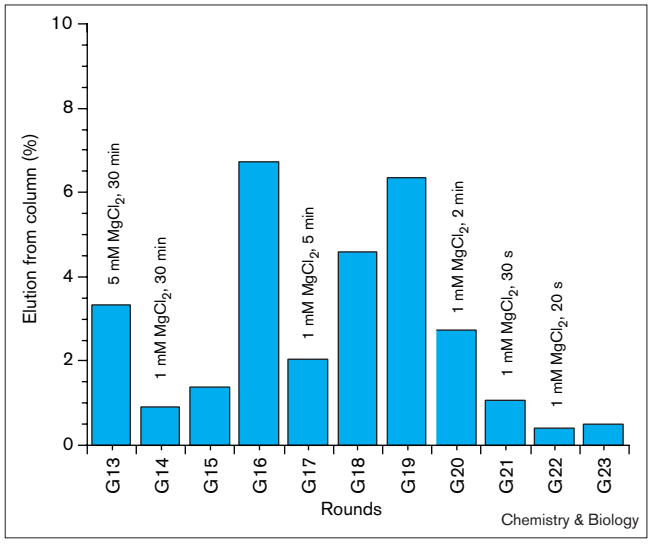

Progress of optimization under physiological conditions (37°C, 50 mM Tris–HCl, pH 7.5, 140 mM KCl, 10 mM NaCl) as measured by column behavior. Percentage of bound pool eluting from column is shown. As signal rose, additional pressure was exerted on the pool in the form of reduced time of exposure to the magnesium-containing elution buffer.

Figure 4

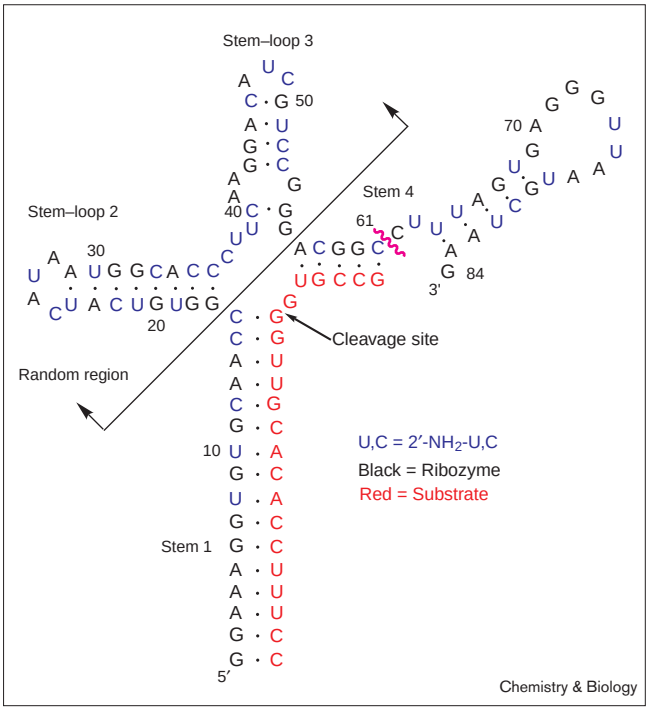

Secondary structure representation of consensus motif (1-9t), cloned from generation 22. Nucleotides 61–84 were part of the primer-binding site for amplification, a potential site of truncation.

were sequenced. From each pool, 36 clones were sequenced and were found to be variations of the same consensus motif (Figure 4, Table 1). RNA from unique clones was assayed for activity in 1 mM $MgCl_2$ and physiological conditions; clone 1-9 represented the consensus sequence and was used in subsequent experiments.

Once selection was completed, we proceeded with initial characterization of the new ribozyme. This included four steps: first, truncations to determine the functional size of the new motif; second, initial kinetic and mechanistic characterization — k_{cat}/K_m, pH and Mg^{2+} dependence of the rate were determined to allow comparison with other ribozymes; third, substrate recognition rules to assess generality in targeting mRNA of interest; fourth, nuclease resistance as a major parameter for *in vivo* applications.

Initial characterization of new ribozyme motif

To make the motif shorter, we deleted the 3′-terminal 25 nucleotides necessary to bind the primer for amplification 1-9t. The measured rates of the full-length and truncated molecules were both 0.04 min^{-1} (data not shown); thus, we were able to reduce the size of the motif from 86 to 61 nucleotides (Figure 4).

Single turnover kinetic measurement of 1-9t in physiological conditions on an 18-mer substrate (binding arms 5/12) is shown in Figure 5. The k_{cat} of this ribozyme is $0.0319 \pm 0{,}0007$ min^{-1} and K_m is 8.67 ± 0.89 nM (close to the 3 nM K_d measurement for pool RNA in the absence of $MgCl_2$), giving a k_{cat}/K_m measurement of 3.7×10^6 min^{-1} M^{-1}. The 1-9t ribozyme is capable of turnover — with 20-fold excess of substrate, 100 nM ribozyme turns over at a rate of once every 2 h. This slower rate is probably the result of slow product release, as one arm of the ribozyme forms 16 base pairs with the substrate RNA.

This novel ribozyme catalyzes cleavage of a specific phosphodiester bond; the resultant products contain a 2′,3′-cyclophosphate and a 5′-OH. This was determined in two ways. First, the 5′ product, a 5′-^{32}P-6-mer, was run on a 20% sequencing gel with both alkaline ladder and RNase T1 ladder. The product had the same migration as fragments in the ladders, which contain 2′,3′-cyclophosphates. Second, we were able to kinase the 3′-16-mer product, indicating that it had a free 5′-OH.

The 1-9t motif has low magnesium dependence (Figure 6) with maximal activity at 2 mM $MgCl_2$, very close to the selection conditions. Using magnesium as the divalent metal, the DNA enzyme shows increasing activity with increasing Mg^{2+} concentrations in a simulated physiological buffer (as measured out to 300 mM $MgCl_2$ in 50 mM EPPS pH 7.5, 150 mM NaCl, 37°C) [34]. Interestingly, the hammerhead ribozyme shows a log-linear response to increasing amounts of magnesium (at pH 7.2 in 50 mM MOPS and 0.5 mM spermine, 25°C) [43]. For comparison, we measured the magnesium dependence of the well-characterized Hammerhead 16, in our buffer [44]. Surprisingly, Hammerhead 16 showed reduced magnesium requirements in pseudo-physiological conditions (Figure 6), most likely a result of the higher concentration of monovalent salts [45]. This result is also supported by intracellular cleavage rates by hammerhead ribozymes in the order of 0.1 min^{-1} (A. McCaffrey and O. Uhlenbeck, personal communication) and may be a function of its occurrence in nature. Chemical stabilization of Hammerhead 16 [8], using modifications relevant to therapeutic ribozymes in clinical trials, reduces cleavage activity *in vitro* (Figure 6) and demonstrates magnesium dependence to be similar to that shown in previous studies [43].

This ribozyme, 1-9t, also showed distinct pH dependence of cleavage rates (Figure 7). Below pH 7.0, the motif is inactive, which is not suprising given the pK_a of the 2′-amino group (pK_a = 6.5) in 2′-deoxy-2′aminouridine and cytidine [41]. Between pH 7.0 and pH 9.0, there is a linear response in activity with a slope of 0.5. Although it has been suggested that a single deprotonation occurs with the hammerhead ribozyme mechanism (a slope of 0.7 that was considered to be sufficiently close to 1) [43] and with the DNA enzyme [34], the slope observed for the 1-9t

Table 1

Random region alignments/mutations.

Position

Clone (No.)	17			20											30										40										50						56	K_{rel}
1-9 motif (42)	G	G	U	G	U	C	A	U	C	A	U	A		A	U	G	G	C	A	C	C	C	U	U	C	A	A	G	G	A	C	A	U	C	G	U	C	C	G	G	G	1.01
1.1 (39)			A*																U*																							0.89
1.6																																		A								1.06
1.27			A*		C														U*																							0.95
1.14 (8)																	A																									0.82
1.16 (5)			A*								C								U*																							0.66
1.20.			A*		A														U*									A														0.61
1.24													U	G																												0.75
1.30.			A*																U*															U								0.81
2.1					C			C																																		0.24
2.13			A*																U*											G												0.19
2.18 (3)			A																A																							0.02
2.34																	A					A																				0.62
2.21															C		A						C																			0.25
2.23 (2)										U																																0.9
2.27			A*		C		G												U																							0.78
2.31																																		U								1.1
2.35			A*		C			C											U*																							0.84
2.36			A*																U*			A																				0.31
2.38 (2)			A*											G					U*																							0.81
2.45 (2)			A*					C											U*																							0.36
3.3								C						G																												0.6
3.6								A									A																									1.11
3.7			A*					C									A		U*																							0.98
3.9																																					U					0.86
3.26			A*					C											U*																							1.51
3.27 (2)																			U																							0.22
3.28 (2)										G																																1.1
4.13 (3)			A*														A		U*																							0.95
4.19																						A																				0.44
4.34 (2)			A*																U*			C																				0.27
4.38 (3)																																C										0.97

Alignment of the random region from 134 clones from generation 22 (1.x = N40, 2.x = N40M, 3.x = N40H, 4.x = N40HM). The number of copies of each mutant is in parentheses. Deviations from the consensus sequence are shown. Mutations that maintain base pair U19–A34 are marked with an asterisk. Activity in single turnover kinetic assay is shown relative to G22 pool rate (50 mM Tris–HCl, pH 7.5, 140 mM KCl, 10 mM NaCl, 1 mM $MgCl_2$, 50 nM ribozyme, trace substrate, 37°C).

motif is too low for a single deprotonation event to explain the mechanism of activity.

Secondary structure, substrate recognition rules and nuclease resistance

Several lines of evidence support the overall secondary structure of 9-1t clone represented in Figure 4, originally derived from the Zuker fold [46]. Analysis of phylogenic data on 134 clones demonstrated that no mutations significantly increased activity; most of the mutations were in regions believed to be duplex, based on the proposed secondary structure (Figure 4, Table 1). Quite characteristic are mutations in proposed base pair U19–A34. Mutations that maintain this base pair U19–A34 supports ribozyme activity (K_{rel} = 1.01); mutations that do not support this base pair (A19–A34 and U19–U34), and therefore can destabilize stem 2 close to what may be catalytic core (G17–C36; C37–A42; G54–G56), are detrimental to cleavage activity (K_{rel} = 0.02 and 0.22, respectively). Additional examples of compensatory mutations in stem 2 can be found in positions (base pairs) U21–G32 and A23–U30. In general, we did not observed many mutations that support activity in the stem–loop 3 region, indicating that this part of the ribozyme is more conserved and may be a part of a catalytic core rather than a supporting structural aliment. A C52→U52 mutation that maintains proposed base pair G44–C52 is well tolerated, as are mutations in the loop (C49→U or A).

The 2′-amino-2′-deoxy C is absolutely required for catalytic activity; an all-ribo-substituted 1-9t does not have any cleavage activity *in vitro*. Substitution of ribo-U during transcription for 2′-amino-2′-deoxy U resulted in a molecule with a tenfold decrease in catalytic rate. In addition, substitution of ribo-C during transcription for 2′-amino-2′-deoxy C resulted in a completely inactive molecule. It is notable that a stretch of 2′-NH_2-pyrimidine nucleotides

Figure 5

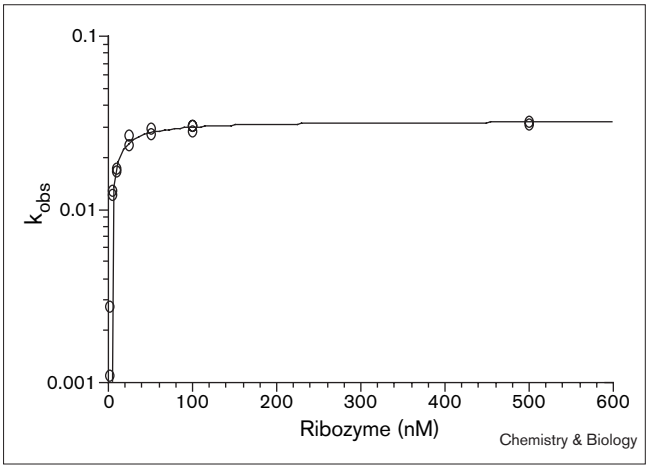

Single-turnover kinetic measurement of the 1-9t motif. Using the Michaelis–Menten equation, $k_{cat} = 0.032 \pm 0.0007$ min^{-1} and $K_m = 8.67 \pm 0.89$ nM. Reaction conditions: 50 mM Tris-HCl, pH 7.5, 140 mM KCl, 10 mM NaCl, 1 mM $MgCl_2$, 5 nM '5/12' substrate (5′-GCCGU G GGUUGCAC ACCU-3′), 37°C.

Figure 7

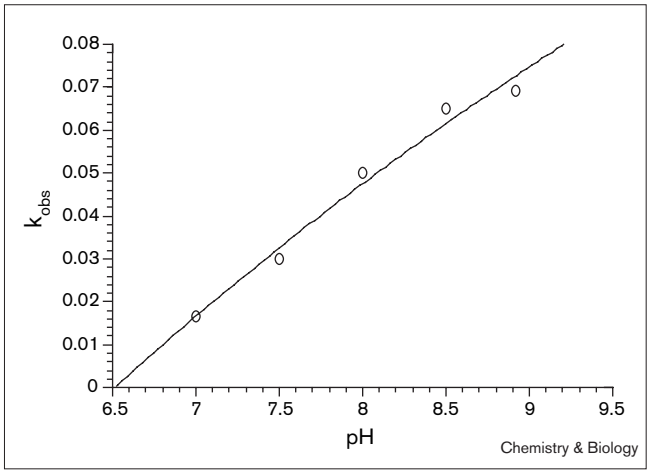

Dependence on pH of 1-9t motif. Linear curve fit gives a slope of 0.53. Single turnover kinetics: 50 mM buffer, 140 mM KCl, 10 mM NaCl, 1 mM $MgCl_2$, 100 nM 1-9t ribozyme, 5 nM '5/12' substrate (5′-GCCGU G GGUUGCAC ACCU-3′), 37°C. pH 7.0–8.5 with Tris–HCl as buffer; pH 8.92 with CHES as buffer. Activity was also tested at pH 6.0 and 6.5 (with MES as buffer) and there was no detectable cleavage.

C36–C40 is a part of highly conserved sequence situated in a four-way junction across from the cleavage site guanosine. Interestingly, it was hypothesized recently, based on crystal structure determination [47] and imidazole rescue experiments [48], that the cytosine base at position 76 of the HDV ribozyme is directly involved in a chemical step of the cleavage mechanism of this ribozyme.

Figure 6

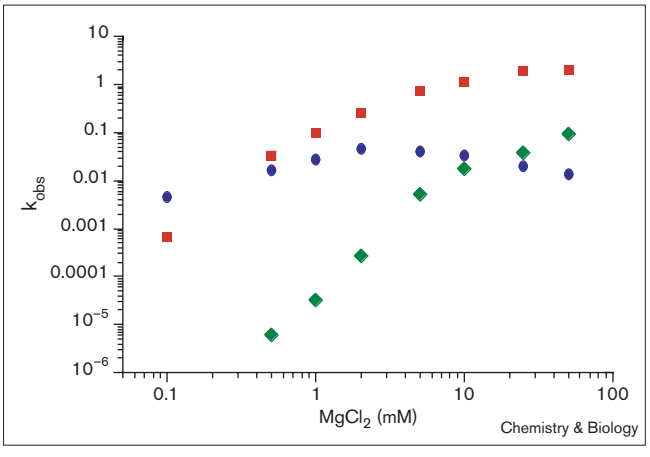

Magnesium dependence of 1-9t motif (circles), hammerhead 16 (HH16; squares) and chemically stabilized HH16 (diamonds). Conditions for single turnover assay: 50 mM Tris–HCl, pH 7.5, 140 mM KCl, 10 mM NaCl, 100 nM ribozyme, 5 nM substrate, 37°C. '5/12' substrate (5′-GCCGU G GGUUGCAC ACCU-3′) was used for 1-9t. HH16 = 5′-GCG AUG ACC UGA UGA GGC CGA AAG GCC GAA ACG UUC CC-3′; HH16 substrate = 5′-GGG AAC GUC GUC GUC GC-3′; chemically stabilized HH16 = 5′-$g_s c_s g_s$ $a_s$ug acc *U*GA uGa ggc cga aag gcc Gaa Acg uuc cc**B** (lower case = 2′-O-methyl nucleotide, upper case = ribonucleotide, *U* = 2′-C-allyl nucleotide, $_s$ = phosphorothioate linkage, **B** = 3′-3′ inverted abasic).

We also explored the effects of possible truncations in the stem–loop 2 and stem–loop 3 structures (Figure 8). Truncation of three base pairs in stem–loop 2, with retention of the original AUAC loop or replacement with a more stable GAAA tetraloop, resulted in a 2–4-fold reduction of activity. It is also possible to truncate an additional base pair with the addition of GAAA tetraloop (K_{rel} = 0.23). Application of the same strategy for truncation of stem–loop 3 while maintaining a full-length stem–loop 2 appeared to be more challenging. Deletion of two distal base pairs with the original AUC triloop retained resulted in more than tenfold decrease in activity. We therefore substituted the AUC triloop in the original motif with a standard GAAA tetraloop in anticipation that this should stabilize the four base pair stem–loop 3 structure. This change allowed subsequent truncation of one (K_{rel} = 1.13) and even two base pairs (K_{rel} = 0.78) in stem–loop 3.

Initial characterization of substrate recognition rules for the 1-9t motif was tested by systematic replacement of base pairs 3′ and 5′ of the cleavage site G, as well as by investigation of the cleavage site nucleotide requirements in wild type 1-9t. The requirements for the cleavage site guanosine nucleotide are rather strict: only uridine is tolerated, but with sixfold decrease in cleavage activity. At the same time, there are no strict sequence requirements for

Figure 8

Representation of stem truncation and loop replacement analysis. K_{rel} is for the 61-mer 1-9t, measured as described in Table 2.

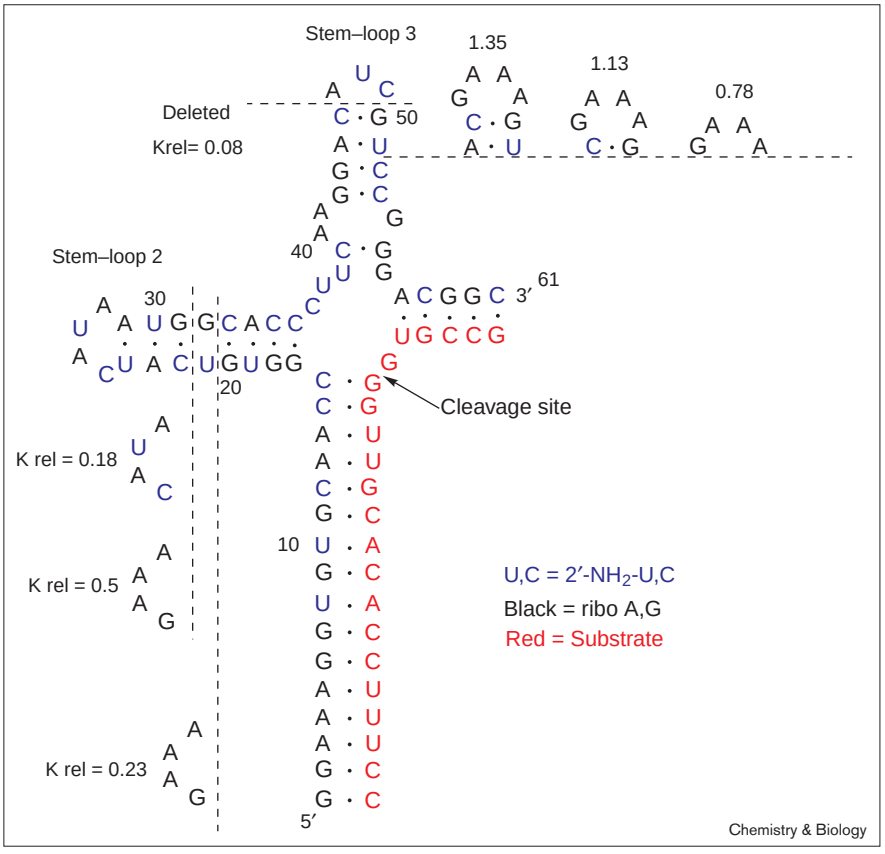

base pairs surrounding the cleavage site G (Table 2), only slight preferences for pyrimidine bases both 3′ and 5′ of the cleavage site.

By design, the 1-9t motif contained asymmetric binding arms (16 and 5) as required by the selection scheme. Truncation of the 'long' arm from 16 to 10 nucleotides did not disrupt cleavage activity (Table 2), indicating that the ribozyme function was not dependent on arm length greater than 10 base pairs. Furthermore, complete replacement of the substrate sequence with corresponding base pairs maintaining changes in recognition arms resulted in fully active ribozyme, confirming its general utility.

Stability of the motif was measured in human serum using a chemically synthesized version of 1-9t. This version contained a 3′–3′ inverted abasic deoxynucleotide at the 3′ end of the molecule. The half-life of synthetic 1-9t was 15.5 h, and results showed protection of the pyrimidine residues to nuclease (Figure 9). Very few degradation products were seen; rather, there was a disappearance of counts over time. Unstabilized hammerhead ribozymes show immediate degradation in human sera [4]; modified hammerhead ribozymes show prolonged half-life in serum. The DNA enzyme, with no modifications, shows degradation products as early as 5 min [35,37]; addition of modifications increased stability.

One should realize that nuclease stabilization against human sera represents only the first step toward a therapeutic ribozyme. Extensive studies on *in vivo* pharmacokinetic of antisense oligonucleotides [49] and stabilized hammerhead ribozyme [50] demonstrated that although sera stability is predictive for *in vivo* behavior, additional stabilization is often required. In particular, 3′ and 5′ modifications as well as additional stabilization of remaining ribo- or deoxy-positions through backbone (monothioate or dithioate) or 2′ modifications can significantly improve *in vivo* stability and pharmacological profile of the target molecules.

Selection of new ribozyme motifs utilizing modified nucleoside 5′-triphosphates

It is well recognized that, despite impressive credentials, RNA and DNA enzymes are not yet as effective catalysts as protein enzymes. Narlikar and Herschlag discussed several explanations of this phenomenon in their comprehensive and insightful review [51]. In their summary, they emphasized that the low diversity of RNA/DNA sidechains, as well as the high charge and flexibility of

Table 2

Substrate requirements for 1-9t motif.

Substrate sequence	1-9t mutation	k_{rel}
5′-GCCGU G GGUUGCAC ACCUUUCC-3′	wt	1.00
5′-GCCG**U** G GGUUGCAC ACCUUUCC-3′	A57G	2.5
5′-GCCG**A** G GGUUGCAC ACCUUUCC-3′	A57U	0.24
5′-GCCG**C** G GGUUGCAC ACCUUUCC-3′	A57G	0.66
5′-GCCG**G** G GGUUGCAC ACCUUUCC-3′	A57C	0.57
5′-GCCGU **U** GGUUGCAC ACCUUUCC-3′	wt	0.17
5′-GCCGU **A** GGUUGCAC ACCUUUCC-3′	wt	n.d.
5′-GCCGU **C** GGUUGCAC ACCUUUCC-3′	wt	n.d.
5′-GCCGU G GGUUGCAC ACCUUUCC-3′	C16U	0.98
5′-GCCGU G **U**GUUGCAC ACCUUUCC-3′	C16G	n.d.
5′-GCCGU G **U**GUUGCAC ACCUUUCC-3′	C16A	0.65
5′-GCCGU G **A**GUUGCAC ACCUUUCC-3′	C16U	0.45
5′-GCCGU G **C**GUUGCAC ACCUUUCC-3′	C16G	0.73
5′-GCCGU G GGUUGCAC ACCUUU-3′	wt	0.89
5′-GCCGU G GGUUGCAC ACCU-3′	wt	1.0
5′-GCCGU G GGUUGCAC AC-3′	wt	0.67

Substrates maintained Watson–Crick or wobble base pairing with mutant 1-9t constructs. Activity in single turnover kinetic assay is shown relative to wild type 1-9t (wt) and 22-mer substrate (reaction conditions: 50 mM Tris–HCl, pH 7.5, 140 mM KCl, 10 mM NaCl, 1 mM $MgCl_2$, 100 nM ribozyme, 5 nM substrate, 37°C). n.d., not determined.

phosphodiester backbone that result in RNA/DNA's compromised ability to create an extensive hydrophobic pocket(s) of low dielectric and limited rigidity to achieve precise positioning are among major factors contributing to deficiency of RNA/DNA-based enzymes compared with protein enzymes.

A straightforward way to address these shortcomings seems to be the addition of a new 'protein-like' functionalities to RNA/DNA utilizing modified nucleoside triphosphates suitable for *in vitro* selection protocols [52]. However, practical realization of this seemingly simple idea has so far achieved only limited success. To date, only two selections with modified triphosphates have produced new catalysts. Eaton and coworkers [53] reported selection of RNA amide synthase with a rate enhancement factor of 10^4 over the uncatalyzed reaction. In this selection, they used 5-imidazole-UTP instead of UTP and the catalytic core of selected enzyme contained three 5-imidazole–uridine nucleotides. The substitution of these conserved modified uridine residues for UTP abolished ribozyme activity. Another report from Eaton's group [54] disclosed successful selection of the RNA ribozyme catalyzing carbon–carbon bond formation in Diels–Alder reaction with 800-fold rate enhancement. In this case, 5-pyridylmethylcaboxamide–UTP was utilized as a modified triphosphate instead of UTP, and earlier selection attempts without this modified nucleotide were unsuccessful [55]. Recent development of the series of

Figure 9

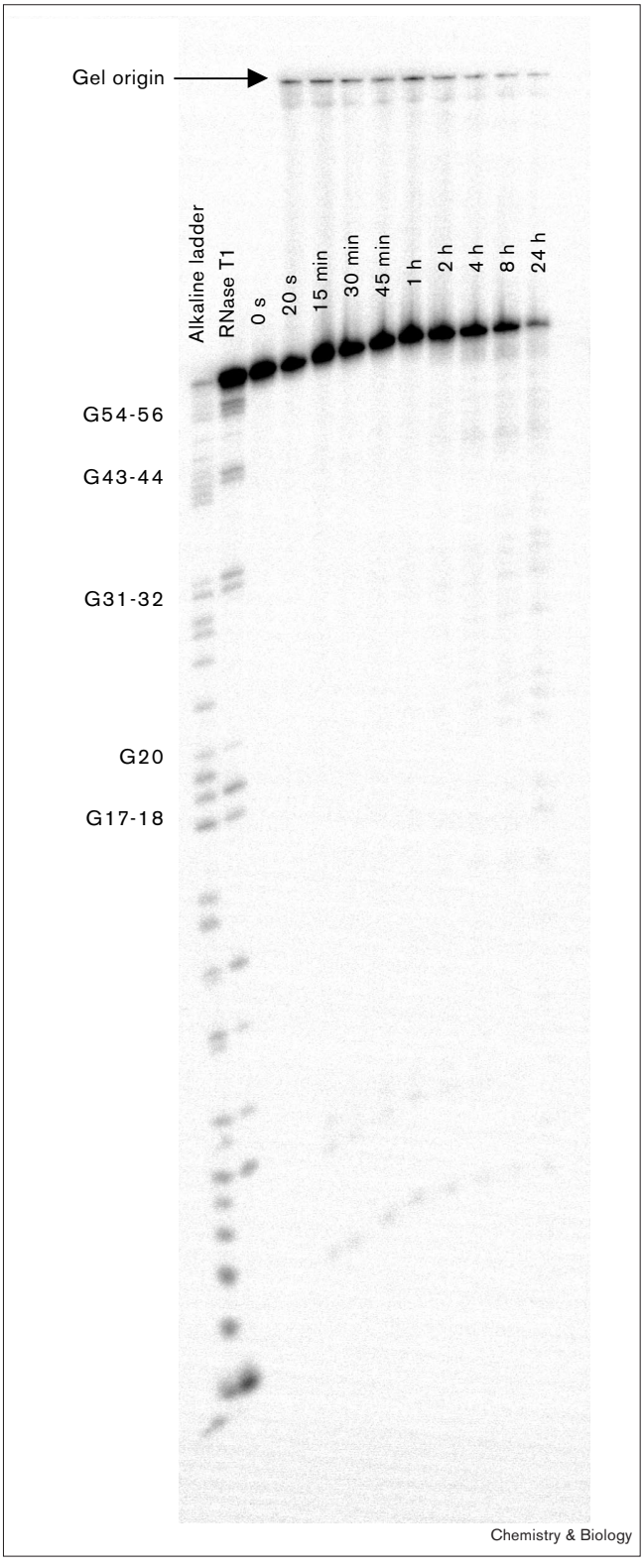

Serum stability analysis of synthetic 1-9t motif. The assay was performed as described in the Materials and methods section. RNase T1 ladder shows position of G residues.

highly functionalized dUTP derivatives that are substrates for thermostable DNA polymerases may yield new catalysts soon [56].

Interestingly, only C-5 pyrimidine or C-8 purine modified nucleoside triphosphates have been utilized to date for the selection of the ribozyme motifs [57]. The chemistry of functionalization for these positions of nucleic acid bases is well developed and such substitutions are well tolerated with polymerases utilized in *in vitro* selection protocols. Unfortunately, modifications at these positions of nucleotides in RNA and/or DNA usually do not improve nuclease resistance.

We decided to search for new nuclease-resistant phospodiesterases in 2′-NH2-C,U modified sequence space for the following reasons: first, 2′-NH2-C,U modification is known to confer nuclease resistance to RNA, and related nucleoside triphosphates are compatible with *in vitro* selection protocol [4,39]; second, because amines react faster than alcohols with phosphoryl compounds but form less stable adducts [58], there is a potential for more rapid turnover in phosphoryl transfer through transient covalent catalysis in 2′-NH2-C,U background; and third, the 2′-NH2-C,U modified RNA forms duplexes with lower thermodynamic stability than unmodified RNA [41]. Therefore, 2′-NH2-C,U modified RNA should be less prone to form stable alternative folds, and even if these alternative conformers form, they can revert to the active conformation with less energetic penalty than unmodified RNA [59]. On the other hand, 2′-NH2-C,U background may require more sequence space to support thermodynamically stable structural elements needed for the formation of a catalytic core and precise positioning during catalysis.

The nuclease resistance of the 1-9t motif in human serum clearly highlights the advantages of using 2′-NH2-U,C modifications versus unmodified pools for *in vitro* selection of nuclease-resistant ribozymes. On the basis of currently available structural and kinetic data it is difficult to conclude whether the 1-9t motif takes full advantage of the present 2′-NH2 functionality for its catalytic mechanism. The fact that ribozyme loses cleavage activity when CTP is substituted for 2′-NH2-CTP indicates absolute requirements for 2′-NH2 functionality of cytidine residues; however, we cannot distinguish if these groups are directly involved in catalysis or play a critical structural role.

The catalytic efficiency of the 1-9t ribozyme ($k_{cat}/K_m = 3.7 \times 10^6$ min^{-1} M^{-1}) measured at 'physiological conditions' is close to that of the optimized all-RNA hammerhead ribozyme. The parity with the hammerhead may result from the incapability of 1-9t to take full advantage of amino functionality under exerted selection pressure. It is also possible that diminished thermodynamic stability of 2′-NH2-U,C containing duplexes may offset potential catalytic advantages offered by this functionality.

In the proposed secondary structure of the 1-9t ribozyme (Figure 4, two stem–loops 'clamping' conserved catalytic core dictate greater sequence requirements for supporting structural elements than compared with the hammerhead, with one stem loop). At the same time, the number of absolutely conserved residues (11–13 nucleotides) is the same for the 1-9t motif (C17, C36–A42, G44–G46, possibly G43 with C53) and hammerhead. Because 2′-NH2-group of uridine residues is not required for catalysis, it is tempting to speculate that performing selection in 2′-F-U, 2′-F-A and 2′-NH2-C background may provide a smaller motif with similar catalytic rates or a motif of the same size but faster rates, which will take advantage of the increased thermodynamic stability of 2′-F-U,A containing duplexes and 2′-NH2 functionality of cytidine residues.

It is also worth noting that all phosphodiester cleaving ribozymes evolved to date by *in vitro* selection process, even the one that utilizes histidine as a cofactor [60], can not achieve a k_{cat} of more than 0.1–0.2 min^{-1} at physiological conditions. What can be done to allow RNA/DNA play 'with the fuller deck' [61] and evolve into more robust, small and nuclease-resistant phosphodiesterases?

In addition to the insightful suggestions summarized by Joyce [61], we believe that it is necessary to develop new polymerizing enzymes that will allow to incorporate a greater variety of modified triphosphates. In particular, enzymes that would be able to incorporate triphosphates with a combination of 2′ modifications, conferring nuclease resistance, and functional modifications, projecting desired groups (such as imidazole and carboxylate) from C-4′ or C-5′ of the sugar moiety and/or C-2 of the purine base, in addition to C-5 and C-8 modifications, are highly desirable. It is also important to develop new selection strategies that would allow to 'catch' and amplify really fast winners without using the manual techniques that currently limit sampling time to 0.5–1 min.

Significance

We have demonstrated that nuclease-resistant ribozymes can be directly evolved through *in vitro* selection. By using 2′-amino-pyrimidine triphosphates and a T7 RNA polymerase, nuclease-stable ribozymes were generated. By imposing desired selective pressure, we were able to find a new motif that had optimal activity in simulated physiological conditions. Moreover, this motif showed minimal substrate recognition rules allowing for a wide range of potential targets. The 1-9t motif was shown to be amenable to truncation through rationally designed deletion analysis. Application of the 1-9t motif to human pathological disease models will be indicative

of the need to perform selections in a physiological environment if a therapeutic nucleic acid enzyme is desired.

The scope of nucleic acid phosphodiester cleavers now includes ribozymes, DNA enzymes, 2′-amino ribozymes, and derived chemically stabilized hybrid molecules. The success of the *in vitro* selection approach has enabled the exploration of new sequence space and chemical functionality. Utilizing novel modifications of nucleoside triphosphates and polymerases with relaxed specificities, many more new catalysts will probably be found. The only limit will be in what modification can survive the constraints of the polymerases necessary for *in vitro* selection.

Materials and methods

Oligonucleotides

DNA oligonucleotides were synthesized by Operon Technologies. Template oligos were purified by denaturing polyacrylamide gel electrophoresis (PAGE) and Sep-pak (Waters) chromatography columns. RNA substrate oligos were synthesized at RPI, purified by denaturing PAGE and ethanol precipitated. Substrates were 5′-end labeled with gamma-^{32}P-ATP and T4 polynucleotide kinase followed by denaturing PAGE purification and ethanol precipitation.

Pool preparation

The initial pool DNA was prepared by converting the template oligo into double-stranded DNA by fill-in with a Taq polymerase. (Template = 5′-ACC CTC ACT AAA GGC CGT (N)40 GGT TGC ACA CCT TTC-3′; primer 1 = 5′-CAC TTA GCA TTA ACC CTC ACT AAA GGC CGT-3'; primer 2 = 5′-TAA TAC GAC TCA CTA TAG GAA AGG TGT GCA ACC-3′.) 5 nmole of template, 10 nmole of each primer and 250 U Taq polymerase were incubated in a 10 ml volume with 1 × PCR buffer (10 mM Tris-HCl, pH 8.3, 1.5 mM $MgCl_2$, 50 mM KCl) and 0.2 mM of each dNTP as follows: 94°C, 4 min; (94°C, 1 min; 42°C, 1 min; 72°C, 2 min) × 4; 72°C, 10 min. The product was analyzed on 2% separide agarose gel for size and extracted twice with buffered phenol, then chloroform-isoamyl alcohol, and ethanol precipitated. The initial RNA pool was made by transcription of 500 pmole (3×10^{14} molecules) of this DNA as follows. Template DNA was added to 40 mM Tris-HCl (pH 8.0), 12 mM $MgCl_2$, 5 mM dithiothreitol (DTT), 1 mM spermidine, 0.002% Triton X-100, 1 mM LiCl, 4% PEG-8000, 10% methanol, 2 mM ATP, 2 mM GTP, 2 mM 2′-amino-dCTP, 2 mM 2′-amino-dUTP, 5 U/ml inorganic pyrophosphatase and 5 U/μl T7 RNA polymerase at room temperature in for a total volume of 1 ml. A separate reaction contained a trace amount of α-^{32}P-GTP for detection. Transcriptions were incubated at 37°C for 2 h followed by addition of equal volume STOP buffer (94% formamide, 20 mM EDTA, 0.05% bromophenol blue). The resulting RNA was purified on a 6% denaturing PAGE gel, followed by Sep-pak chromatography and ethanol precipitation.

Initial selection

2 nmole of 16 mer 5′-biotinylated substrate (5′-biotin-C18 linker-GCC GUG GGU UGC ACA C-3′) was linked to 200 μl UltraLink immobilized NeutrAvidin resin (400 μl slurry, Pierce) in binding buffer (20 mM Na_3PO_4, pH 7.5, 150 mM NaCl) for 30 min at room temperature. The substrate column was washed with 2 ml binding buffer followed by 2 ml column buffer (50 mM tris-HCl (pH 8.5), 100 mM NaCl, 50 mM KCl). 1000 pmole of initial pool RNA in 200 μl column buffer was added to the resin and incubated for 30 min at room temperature. The column was subsequently washed with 2 ml column buffer. 200 μl elution buffer (column buffer + 25 mM $MgCl_2$) was added to the column and allowed to incubate 30 min at room temperature. Eluent was collected followed by three 200 μl elution buffer washes. The eluent/washes were ethanol precipitated using 80 μg glycogen as carrier and rehydrated in 50 μl sterile H_2O. The eluted RNA was amplified by reverse transcription/PCR. 5–31 μl RNA was incubated with 20 pmol of primer 1 in 14 μl, at volume 90°C for 3 min, then placed on ice for 1 min. The following reagents were added (final concentrations noted): 1 × PCR buffer, 1 mM each dNTP, 2 U/μl RNase Inhibitor, 10 U/μl SuperScript II reverse transcriptase. The reaction was incubated at 42°C for 1 h followed by 95°C for 5 min to inactivate the reverse transcriptase. The volume was then increased to 100 μl by adding water and reagents for PCR: 1 × PCR buffer, 20 pmol primer 2 and 2.5 U Taq DNA polymerase. The reaction was cycled in a Hybaid thermocycler: 94°C, 4 min; (94°C, 30 sec; 54°C, 30 sec; 72°C, 1 min) × 25; 72°C, 5 min. Products were analyzed on agarose gel for size and ethanol precipitated. One-third to one-fifth of the PCR DNA was used to transcribe the next generation, in a 100 μl volume, as described above. Subsequent rounds used 20 pmol RNA for the column with 40 pmol substrate.

Two column selection

At generation 8, the column selection was changed to a two column format. 200 pmoles of 22-mer 5′-biotinylated substrate (5′-biotin-C18 linker-GCC GUG GGU UGC ACA CCU UUC C-C18 linker-thiol modifier C6 S-S-inverted abasic-3′) was used in the selection column as described above. Elution was in 200 μl elution buffer followed by a 1 ml elution buffer wash. The 1200 μl eluent was passed through a product trap column by gravity. The product trap column was prepared as follows: 200 pmol 16 mer 5′-biotinylated 'product' (5′-GGU UGC ACA CCU UUC C-C18 linker-biotin-3′) was linked to the column as described above and the column was equilibrated in elution buffer. Eluent from the product column was precipitated as previously described. The products were amplified as above only with 2.5 times more volume and 100 pmol each primer. 100 μl of the PCR reaction was used to do a cycle course; the remaining fraction was amplified the minimal number of cycles needed for product.

Cloning and sequencing

Generations 13 and 22 were cloned using Novagen's Perfectly Blunt Cloning kit (pT7Blue-3 vector) following the kit protocol. Clones were screened for insert by PCR amplification using vector-specific primers. Positive clones were sequenced using ABI Prism 7700 sequence detection system and vector-specific primer. Sequences were aligned using MacVector software; two-dimensional folding was done using Mulfold software [46]. Individual clone transcription units were constructed by PCR amplification with 50 pmol each of primer 1 and primer 2 in 1 × PCR buffer, 0.2 mM each dNTP and 2.5 U of taq polymerase in 100 μl volume cycled as follows: 94°C, 4 min; (94°C, 30 s; 54°C, 30 s; 72°C, 1 min) × 20; 72°C, 5 min. Transcription units were ethanol precipitated, rehydrated in 30 μl H_2O and 10 μl was transcribed in 100 μl volume and purified as previously described.

Kinetic analysis

Single turnover kinetics were performed with trace amounts of 5′-^{32}P-labeled substrate and 10–1000 nM pool or ribozyme. 2 × substrate in 1 × buffer and 2 × pool/ribozyme in 1 × buffer were incubated separately at 90°C for 3 min followed by equilibration to 37°C for 3 min. Equal volume of 2 × substrate was added to pool/ribozyme at t_0 and the reaction was incubated at 37°C. Time points were quenched in 1.2 volume of STOP buffer on ice. Samples were heated to 90°C for 3 min prior to separation on 15% sequencing gels. Gels were imaged using a phosphorimager and quantitated using ImageQuant software (Molecular Dynamics). Curves were fit to double-exponential decay in most cases, although some of the curves required linear fits.

Gel shift analysis

K_d was measured by gel shift analysis in pool/ribozyme excess [62,63]. 2 × ribozyme/pool was incubated for 3 min at 25°C in 50 mM Tris–HCl (pH 8.5), 100 mM NaCl, 50 mM KCl, 5% sucrose, 0.02% bromophenol blue, and 0.02% xylene cyanol. 2 × ^{32}P-substrate or product (trace) was incubated in the same conditions separately. Equal volume 2 × substrate or product was added to the ribozyme/pool tube and allowed

to equilibrate at 25°C for 30 min. The complex was loaded onto a 12% nondenaturing temperature-controlled PAGE gel running at 20 W. The gel and running buffer contained 50 mM Tris-acetate (pH 8.5), 100 mM NaCl, and 50 mM KCl. Gel buffer was recirculated throughout the run by a peristaltic pump to keep pH constant. Ribozyme/pool concentrations over 4 logs were used to determine K_d. Gels were quantitated as described above and curves were fit to theorhetical binding curves.

Ribozyme stability analysis

Briefly, 100 pmoles of starting material was end-labeled with [γ-^{32}P]ATP. This end-labeled material was combined with 500 pmoles of unlabeled (cold) ribozyme. The mixture was dried down and resuspended in 20 µl of fresh 100% human serum. The suspension was incubated at 37°C for 23.3 h. Aliqouts (2 µl) of the reaction were removed at 0, 0.25, 0.5, 0.75, 1, 2, 4, 8 and 23.3 h. The reaction aliquots were immediately quenched by removal into 5 µl of 95% formamide, 20 mM EDTA, 0.05% bromphenol blue and 0.05% xylene cyanol on ice. A portion of each time point was counted in a scintillation counter for normalizing counts per lane. The time points were heated to 95°C for 1 min and loaded onto a denaturing 20% polyacrylamide gel at 10^6 cpm per lane. Intact ribozyme and the specific RNA degradation products generated by exposure to ribonucleases in the serum were visualized by scanning a phosphorimager screen which had been exposed to the assay gel. The fraction of full-length ribozyme at each time point was determined by phosphor imager quantitation of bands representing the intact ribozyme and it's degradation products.

References

1. Kruger, K., Grabowski, P.J., Zaug, A,J., Sands, J., Gottschling, D.E. & Cech, T.R. (1982). Self-splicing RNA: autoexcision and autocyclization of the ribosomal RNA intervening sequence. *Cell* **31**, 147-157.
2. Guerrier-Takada, C., Gardiner, K., Marsh, T., Pace, N. & Altman, S. (1983). The RNA moiety of ribonuclease P is the catalytic subunit of the enzyme. *Cell* **35**, 849-857.
3. Christoffersen R.E. & Marr, J.J. (1995). Ribozymes as human therapeutic agents. *J. Med. Chem.* **38**, 2024-2037.
4. Beigelman, L., *et. al.*, & Usman, N. (1995). Chemical modification of hammerhead ribozymes. *J. Biol. Chem.* **43**, 25702-25708.
5. Paolella, G., Sproat, B.S. & Lamond A.I. (1992). Nuclease resistant ribozyme with high catalytic activity. *EMBO J.* **11**, 1913-1919.
6. Flory, C.M., *et al.,* & Schrier, D.J. (1996) Nuclease-resistant ribozymes decrease stromelysin mRNA levels in rabbit synovium following exogenous deliver to the knee joint. *Proc. Natl Acad. Sci. USA* **93**, 754-758.
7. Jarvis T.C, *et al.,* & Stinchcomb D.T, (1996). Inhibition of vascular smooth muscle cell proliferation by ribozymes that cleave *c-myb* mRNA. *RNA* **2**, 419-428.
8. Parry J.T., *et al.*, & Pavco P.E. (1999). Bioactivity of anti-angiogenic ribozymes targeting Flt-1 and KDR mRNA. *Nucleic Acids Res.* **27**, 2569-2577.
9. Sioud, M. & Sorenson, D.R. (1998). A nuclease-resistant protein kinase C α ribozyme blocks glioma cell growth. *Nat. Biotechnol.* **16**, 556-561.
10. Pyle, A.M. (1993). Ribozymes: a distinct class of metalloenzymes. *Science* **261**, 709-714.
11. Eckstein, F. & Lilley, D.M.J (1997). *Catalytic RNA* (2nd edn), Springer, Berlin.
12. Sigurdsson, S.T., Thomson, J.B. & Eckstein, F. (1998) Small Ribozymes. In *RNA Structure and Function.* (Simons R.W and Grunberg-Manago M, eds.) pp. 339-376. Cold Spring Harbor Laboratory Press, New York.
13. Breaker, R.R. (1998). *In vitro* selection of catalytic polynucleotides. *Chem. Rev.* **98,** 2260-2290.
14. Pan, T. (1997). Novel and variant ribozymes obtained through *in vitro* selection. *Curr. Opin. Chem. Biol.* **1**, 17-25.
15. Lorsch, J.R. & Szostak, J.W. (1996). Chance and necessity in the selection of nucleic acid catalysts. *Accounts Chem. Res.* **29**, 103-110.
16. Joyce, G.F. (1994). *In vitro* evolution of nucleic acids. *Curr. Opin. Struct. Biol.* **4**, 331-336.
17. Joyce, G.F. (1989) Amplification, mutation and selection of catalytic RNA. *Gene* **82**, 83-87.
18. Tuerk, C. & Gold, L. (1990). Systematic evolution of ligands by exponential enrichment: RNA ligands to bacteriophage T4 DNA polymerase. *Science* **249**, 505-510.
19. Ellington A.D. & Szostak J.W. (1990) *In vitro* selection of RNA molecules that bind specific ligands. *Nature* **346**, 818-822.
20. Williams, K.P., Clafre, S. & Tocchini-Valentini, G.P. (1995). Selection of novel Mg^{2+} dependent self-cleaving ribozymes. *EMBO J.* **14**, 4551-4557.
21. Long, D.M. & Uhlenbeck, O. (1994). Kinetic characterization of intramolecular and intermolecular hammerhead RNAs with stem II deletions. *Proc. Natl Acad. Sci. USA* **91**, 6977-6981.
22. Ishizaka, M., Ohshima, Y. & Tani, T. (1995). Isolation of active ribozymes from an RNA pool of random sequences using an anchored substrate RNA. *Biochem. Biophys. Res. Comm.* **214**, 403-409.
23. Nakamaye, K.L. & Eckstein, F. (1994). AUA-cleaving hammerhead ribozymes: attempted selection for improved cleavage. *Biochemistry* **33**, 1271-1277.
24. Thomson, J.B., Sigurdsson, ST., Zeuch, A. & Eckstein, F. (1996). *In vitro* selection of hammerhead ribozymes containing a bulged nucleotide in stem II. *Nucleic Acids Res.* **24**, 4401-4406.
25. Vaish, N.K., Heaton, P.A. & Eckstein, F. (1997). Isolation of hammerhead ribozymes with altered core sequences by *in vitro* selection. *Biochemistry* **36**, 6495-6501.
26. Conaty, J., Hendry, P. & Lockett T. (1999). Selected classes of minimized hammerhead ribozyme have very high cleavage rates at low Mg^{2+} concentration. *Nucleic Acids Res.* **27**, 2400-2407.
27. Zillmann, M., Limauro, S.E. & Goodchild, J. (1997). *In vitro* optimization of truncated stem-loop II variants of the hammerhead ribozyme for cleavage in low concentrations of magnesium under non-turnover conditions. *RNA* **3**, 734-747.
28. Burgin, A.B., *et al.*, & Beigelman, L. (1996). Chemically modified hammerhead ribozymes with improved catalytic rates. *Biochemistry* **35**, 14090-14097.
29. Vaish, N., Heaton, P., Fedorova, O. & Eckstein, F. (1998). *In vitro* selection of a purine nucleotide-specific hammerhead-like ribozyme. *Proc. Natl Acad. Sci. USA* **95**, 2158-2162.
30. Chartrand, P., Harvey, S., Ferbeyre, G., Usman, N. & Cedergren, R. (1995). An oligodeoxyribonucleotide that supports catalytic activity in the hammerhead ribozyme domain. *Nucleic Acid Res.* **23**, 4092-4096.
31. Breaker, R. & Joyce, G. (1994). A DNA enzyme that cleaves RNA. *Chem. Biol.* **1**, 223-229.
32. Breaker, R. & Joyce, G. (1995). A DNA enzyme with Mg^{2+}-dependent RNA phosphoesterase activity. *Chem. Biol.* **2**, 655-660.
33. Santoro, S. & Joyce, G. (1997). A general purpose RNA-cleaving DNA enzyme. *Proc. Natl Acad. Sci. USA* **94**, 4262-4266.
34. Santoro, S. & Joyce, G. (1998). Mechanism and utility of an RNA-cleaving DNA enzyme. *Biochemistry* **37**, 13330-13342.
35. Warashina, M., Kuwabara, T., Nakamatsu, Y. & Taira, K. (1999). Extremely high and specific activity of DNA enzymes in cells with a Philadelphia chromosome. *Chem. Biol.* **6**, 237-250.
36. Cairns, M., Hopkins, T., Witherington, C., Wang, L. & Sun, L. (1999). Target site selection for an RNA-cleaving catalytic DNA. *Nat. Biotechnol.* **17**, 480-486.
37. Sun, L., Cairns, M., Gerlach, W., Witherington, C., Wang, L. & King, A. (1999). Suppression of smooth muscle cell proliferation by a c-*myc* RNA-cleaving deoxyribozyme. *J. Biol. Chem.* **274**, 17236-17241.
38. Huang, Y., Beaudry, A., McSwiggen, J. & Sousa, R. (1997). Determinants of ribose specificity in RNA polymerization: effects of Mn^{2+} and deoxynucleoside monophosphate incorporation into transcripts. *Biochemistry* **36**, 13718-13728.
39. Lin, Y., Qiu, Q., Gill, S. & Jayasena, S. (1994). Modified RNA sequence pools for *in vitro* selection. *Nucleic Acids Res.* **22**, 5229-5234.
40. Freier, S.M., *et al.*, & Turner, D.H. (1986). Improved free-energy parameters for predictions of RNA duplex stability. *Proc. Natl Acad. Sci. USA* **83**, 9373-9377.
41. Aurup, H., Tuschl, T., Benseler, F., Ludwig, J., & Eckstein, F. (1994). Oligonucleotide duplexes containing 2′-amino-2′-deoxycytidines: thermal stability and chemical reactivity. *Nucleic Acids Res.* **22**, 20-24.
42. Vartanian, J., Henry, M. & Wain-Hobson, S. (1996). Hypermutagenic PCR involving all four transitions and a sizeable proportion of transversions. *Nucleic Acids Res.* **24**, 2627-2631.
43. Dahm, S., Derrick, W. & Uhlenbeck, O. (1993). Evidence for the role of solvated metal hydroxide in hammerhead cleavage mechanism. *Biochemistry* **32**, 13040-13045.
44. Hertel, K., Herschlag, D. & Uhlenbeck, O. (1994). A kinetic and thermodynamic framework for the hammerhead ribozyme reaction. *Biochemistry* **33**, 3374-3385.
45. Murray, J., Seyhan, A., Walter, N., Burke, J. & Scott, W. (1998). The hammerhead, hairpin, and VS ribozymes are catalytically proficient in monovalent cations alone. *Chem. Biol.* **5**, 587-595.

46. Zucker, M. (1989). On finding all suboptimal foldings of an RNA molecule. *Science* **244**, 48-52.
47. Ferre-D'Amare, A.R., Zhou, K. & Doudna, J.A. (1998). Crystal structure of a hepatitus delta virus ribozyme. *Nature* **395**, 567-574.
48. Perrotta, A.T., I-hung, S. & Been, M.D. (1999). Imidazole rescue of cytosine mutation in a self-cleaving ribozyme. *Science* **286**, 123-126.
49. Agrawal, S., Temsamani, J., Galbraith, W. & Tang, J.Y (1995). Pharmacokineticis of antisence oligonucleotides. *Clin. Pharmacokinet.* **28**, 7-16.
50. Sandberg, J.A, *et al.*, & Parry, T.J. (1999). Pharmacokinetics of angiogenic ribozyme (ANGIOZYME™) in the mouse. *Antisense Nucl. Acid Drug Dev.* **9**, 271-277.
51. Narlikar, G.J. & Herschlag, D. (1997). Mechanistic aspects of enzymatic catalysis: lessons from comparison of RNA and protein enzymes. *Ann. Rev. Biochem.* **66**, 19-59.
52. Tarasow, T.M. & Eaton, B.E. (1998). Dresses for success: realizing the catalytic potential of RNA. *Biopolymers* **48**, 29-37.
53. Wiegand, T.W., Janssen, R.C. & Eaton, B.E. (1997). Selection of RNA amide synthases. *Chem. Biol.* **4**, 675-683.
54. Tarasow, T.M., Tarasow, S.L. & Eaton, B.E. (1997). RNA-catalysed carbon–carbon bond formation. *Nature* **389**, 54-57.
55. Morris, K.N., *et al.*, & Gold, L. (1994). Enrichment for RNA molecules that bind a Diels-Alder transition state analog . *Proc. Natl Acad. Sci. USA* **91**,13028-13032.
56. Sakthivel, K. & Barbas, C.F. III. (1998). Expanding the potential of DNA for binding and catalysis: highly functionalized dUTP derivatives that are substrates for thermostable DNA polymerases. *Angew. Chem. Int. Ed.* **37**, 2872-2875.
57. Perrin, D.M., Garestier, T. & Helene, C. (1999). Expanding the catalytic repertoire of nucleic acid catalysts: simultaneous incorporation of two modified deoxyribonucleoside triphosphates bearing ammonium and imidazolyl functionalities. *Nucleosides Nucleotides* **18,** 377-391.
58. Herschlag, D. & Jencks, W.P. (1989). Phosphoryl transfer to anionic oxygen nucleophiles. Nature of the transition state and electrostatic repulsion. *J. Am. Chem. Soc.* **111**, 7587-7596.
59. Herschlag, D. (1995). RNA chaperones and the RNA folding problem. *J. Biol. Chem.* **270**, 20871-20874.
60. Roth, A. & Breaker, R.R. (1998). An amino acid as a cofactor for a catalytic polynucleotide. *Proc. Natl Acad. Sci. USA* **95**, 6027-6031.
61. Joyce, G.F. (1998) Nucleic acid enzymes: playing with a fuller deck. *Proc. Natl Acad. Sci. USA* **95**, 5845-5847.
62. Pyle, A., McSwiggen, J. & Cech, T. (1990). Direct measurement of oligonucleotide substrate binding to wild-type and mutant ribozymes from Tetrahymena. *Biochemistry* **87**, 8187-8191.
63. Fedor, M. & Uhlenbeck, O. (1992). Kinetics of intermolecular cleavage by hammerhead ribozymes. *Biochemistry* **31**, 12042-12054.